

## An Improved Theoretical Lunar Photometric Function

BRUCE HAPKE

*Cornell-Sydney University Astronomy Center, Cornell University, Ithaca, New York*

(Received 3 January 1966)

The theoretical photometric function for the lunar surface previously proposed by the author, which successfully predicted variations of brightness for areas between selenographic longitudes of  $\pm 60^\circ$ , has been improved so that it better agrees with observations in the limb regions. The modification consists of wrinkling the porous, open surface of the previous model into a series of steep-sided depressions. For formal mathematical reasons, the depressions used are cylindrical troughs whose axes are parallel to lines of luminance longitude. However, the primary requirement is that the surface must be densely covered ( $\sim 90\%$ ) with features whose walls make steep angles ( $\geq 45^\circ$ ) with the local horizontal, and that these walls must be visible even at glancing angles. This model is consistent with radar-reflection data which indicate that the moon is rough on a subcentimeter scale. Hence, the size of these depressions is inferred to be centimeters and millimeters. These features are probably primary and secondary meteorite craters and ejecta debris, which saturate the lunar surface on a small scale.

### I. INTRODUCTION

THE unusual and distinctive photometric properties of the lunar surface are well known. They have been summarized by Minnaert (1962) and by Fessenkov (1962). The most important characteristic of the lunar scattering law is that all areas of the lunar surface are brightest at full moon when the source of illumination is directly behind the observer. This phenomenon is independent of the type of terrain, being a property of maria, highland and ray surfaces as well as of rims of craters and of steep, sloping areas. Hapke and Van Horn (1963), Hapke (1965a,b) and also Rosenberg and Wehner (1964) have reproduced these and other lunar optical properties in the laboratory using fine rock powders darkened by hydrogen ion irradiation to simulate the solar wind bombardment of the lunar surface.

The author (Hapke 1963; hereafter referred to as Paper I) proposed a theoretical photometric function for the lunar surface which successfully predicted the observations of the change of brightness with phase angle except for regions close to the limb. The optical model of the lunar surface used in Paper I consists of an optically thick layer of objects large compared with the wavelength of visible light and arranged in an open, porous network into which light from any direction can penetrate freely. The objects are randomly oriented and located irregularly within the layer. The scattering objects have an albedo sufficiently small that only singly scattered rays of light contribute appreciably to the brightness of the surface. On a scale large compared with the size of the scatterers the surface was taken to be flat and featureless.

The backscattering properties of this layer were then explained in Paper I as being due to two effects. (1) When an observer looks parallel to the direction of incident radiation he sees only fully illuminated surfaces, but when he looks in any other direction he sees surfaces partly illuminated and partly in shadow. Thus the area is brightest when the source and detector are aligned. (2) For a surface riddled with deep tunnels

pointing in all directions, such as the model of Paper I, the direction opposite to that of the incident radiation is a preferred direction for escape of a reflected ray. A bundle of light rays entering the surface will be attenuated by blocking and scattering on its way in, but the light scattered from deep in the interior of the layer and reflected directly back toward the source can escape without attenuation. The same will be true for rays reflected into the small cone about the direction of incidence, the cone of nonattenuation being narrower for rays reflected from deeper under the surface.

These effects were described mathematically in Paper I. In the present paper a relatively minor modification in the model is introduced which extends the agreement of the theoretical function with observations to the limb regions of the moon. The modification consists of wrinkling the macroscopic surface, which was assumed to be flat and horizontal in the old theory, into a series of depressions or other steep-sided features. The implications which this modified model has for the fine-scale structure of the lunar surface are discussed in the last section of the paper. The manner in which the opposition effect (Gehrels *et al.* 1964) can be incorporated into the theoretical function is also discussed.

### II. PHOTOMETRIC FUNCTION

#### A. General Function

It was shown in Paper I that the amount of light received by a detector on the earth scattered from a region on the lunar surface can be written in the form

$$E = E_0 a d \omega (2/3\pi) b \phi(\alpha, \beta, g), \quad (1)$$

where  $E_0$  is the intensity of incident radiation at the surface,  $a$  is the light-sensitive area of the detector,  $d\omega$  is the solid angle of acceptance of the detector,  $b$  is the total reflectivity of a particle of the lunar soil (Bond albedo),  $\phi$  is the photometric function (by definition  $\phi = 1$  when  $g = 0$ ),  $\alpha$  is the luminance longitude,  $\beta$  is the luminance latitude, and  $g$  is the phase angle. The angles  $\alpha$ ,  $\beta$ , and  $g$  refer to the selenographic coordinate system based on the instantaneous positions of the subearth

and subsolar points rather than to a grid system fixed with respect to the lunar surface (it is noted that the notation of this paper is somewhat different from that used in Paper I in order to conform with common usage).

It was shown in Paper I that the photometric func-

tion can be written in the general form

$$\phi(\alpha, \beta, g) = L(\alpha, g) \sum(g) B(g). \quad (2)$$

In Eq. (2)  $B$  is the retrodirective function which describes the backscattering due to the effects of blocking and shadowing within the lunar soil:

$$B(g) = \begin{cases} \left[ 2 - \frac{\tan |g|}{2h} (1 - e^{-h/\tan |g|}) (3 - e^{-h/\tan |g|}) \right], & |g| \leq \frac{1}{2}\pi, \\ 1, & |g| \geq \frac{1}{2}\pi. \end{cases} \quad (3)$$

The parameter  $h$  determines the sharpness of the brightness peak near full moon and is related to the porosity of the lunar soil. The retrodirective function is plotted versus  $g$  for several values of  $h$  in Fig. 1. Most areas on the moon apparently can be described by values of  $h$  between 0.4 and 0.8.

The function  $\sum$  describes the average angular scattering function of a single particle of the lunar soil:

$$\sum(g) = \left[ \frac{(\sin |g| + (\pi - |g|) \cos |g|)}{\pi} + 0.1(1 - \cos |g|)^2 \right]. \quad (4)$$

The first term of (4) is the Schoenberg function, which is the scattering function of a sphere, each of whose elements reflect light in accordance with Lambert's law; the same function also describes the average scattering characteristics of particles of arbitrary shape having rough, diffuse surfaces oriented at random. The Schoenberg function is plotted as curve C in Fig. 2. The

second term of (4) is an empirical forwardscattering term describing light transmitted through the particle. It was found necessary in Paper I to add a term of this type to  $\sum$  in order to match Rougier's curve of the integrated light from the moon. The complete expression for  $\sum$  is plotted as curve A of Fig. 2.

The function  $L$  in (2) is a reflection function describing the effect of surface geometry on the brightness for a surface which is porous on a microscopic scale but whose large-scale topology is a flat horizontal plane;  $L$  is the Lommel-Seeliger law:

$$L(\alpha, g) = \cos(\alpha + g) / [\cos \alpha + \cos(\alpha + g)]. \quad (5)$$

The improvement in  $\phi$  is seen to consist of a modification of the form of  $L$ .

The theoretical function described by Eqs. (1)–(5) agrees with observations of most areas of the lunar surface; this function has the properties of increasing sharply in brightness at full moon, of being independent of selenographic latitude, and at  $g=0$  of being independent of  $\alpha$  and  $\beta$ .

Equations (1)–(5) describe the brightness of that portion of a flat, locally horizontal surface seen by a detector which accepts light from within a small solid angle  $d\omega$ . It was shown in Paper I that the light scattered into the detector from an increment of surface area  $dA$  is

$$dE = E_0 \frac{2}{3\pi} b d\Omega dA \frac{\cos i \cos \epsilon}{\cos i + \cos \epsilon} \sum(g) B(g), \quad (6)$$

where  $d\Omega$  is the solid angle subtended at  $dA$  by the detector,  $\epsilon$  is the angle of observation, and  $i$  is the angle of incidence. For a spherical surface  $\epsilon$ ,  $i$ , and  $d\Omega dA$  are related to  $\alpha$ ,  $\beta$ , and  $ad\omega$  through

$$\cos \epsilon = \cos \beta \cos \alpha, \quad \cos i = \cos \beta \cos(\alpha + g), \quad (7)$$

$$d\Omega dA \cos \epsilon = ad\omega. \quad (8)$$

The differential photometric function (6) was integrated in Paper I over all areas of the lunar sphere which are both visible and illuminated to give an expression for the integrated photometric function of the moon,

$$\Phi(g) = I(g) \sum(g) B(g), \quad (9)$$

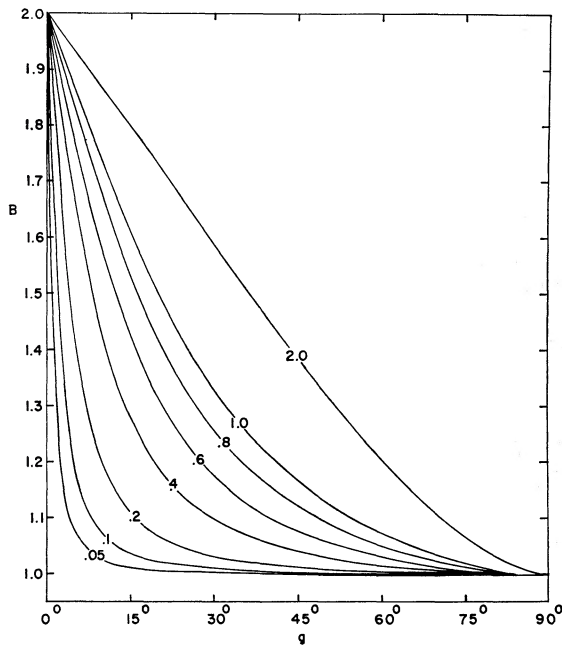


FIG. 1. Retrodirective function versus phase angle for various values of the parameter  $h$ ;  $B(g) = 1$  for  $90^\circ \leq g \leq 180^\circ$ ;  $B(-g) = B(g)$ .

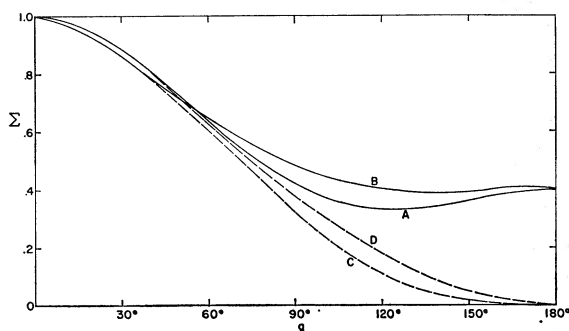


FIG. 2. Angular scattering functions of a single average particle versus phase angle. Curve A: sphere whose surface elements scatter according to the Lambert law plus the forward-scattering term; curve B: sphere whose surface elements scatter according to the Lommel-Seeliger law plus the forward-scattering term; curve C: Lambert law sphere alone (Schoenberg function); curve D: Lommel-Seeliger law sphere alone.

where  $\Sigma$  and  $B$  are given by (3) and (4), respectively, and

$$I(g) = \frac{1}{2} [1 - \sin \frac{1}{2} |g| \tan \frac{1}{2} |g| \ln(\cot \frac{1}{4} |g|)]. \quad (10)$$

### B. Improved Photometric Function

The major discrepancies between the forms of  $\phi$  as given in Paper I and observations of the lunar surface occur at large values of  $|\alpha|$ . For regions with  $|\alpha|$  greater than about  $70^\circ$   $\phi$  is unity at full moon, but as  $g$  increases from zero and the sun moves towards being overhead at these regions,  $\phi$  continues to increase and grows to a broad maximum which is shifted towards local moon. This prediction is in contrast to photometric observations (Fedoretz 1952; Van Diggelen 1958) which show that even the limb regions are brightest at full moon. This anomalous behavior of  $\phi$  is illustrated by the dashed curves of Fig. 3, in which the old  $\phi$  has been plotted versus  $\alpha$  for a few positive values of  $g$ .

In Paper I it was suggested that the limb discrepancy was due to the model incorrectly specifying the manner in which the density of scattering particles of lunar soil changes at the apparent surface. The model has the particle density changing everywhere in step fashion from zero to full value at the interface, whereas it was thought that on the moon the change would be more gradual. However, the foregoing cannot be the cause of the incorrect behavior of  $\phi$  because such an effect would be apparent for  $|\beta|$  near  $90^\circ$  as well as when  $|\alpha|$  is near  $90^\circ$ . Furthermore, the discrepancy cannot be removed by altering either  $\Sigma$  or  $B$  (for instance by choosing a smaller value of the sharpness parameter  $h$ ), since such action would cause the agreement with observations near the center of the lunar disk to become poor. Hence a re-examination of the form of  $L$  is necessitated.

An obvious oversimplification in Paper I was the assumption that the macroscopic surface is locally flat and horizontal. If the Ranger pictures are represen-

tative of the moon's surface, the lunar topography appears to be dominated by craters. Also, radar studies indicate that on a scale larger than a few centimeters the surface of the moon is smooth and gently undulating, but that on a smaller scale the surface is rough (Evans and Hagfors 1964). It is intuitively apparent that distorting the surface from local flatness will decrease the limb brightness, for if surfaces which are tilted toward the observer are visible in the limb regions their brightness will be the same as that of a surface which is located at a smaller longitude.

A number of types of distortion of the surface were initially considered. Most were rejected either because of analytical difficulties or because the resulting brightness curves did not match the lunar observations. For instance, domes or other structures which are convex-upward are not capable of reducing the limb brightness, because when viewed nearly parallel to the surface mainly the tops of the structures are visible and these tops are horizontal; thus the limb brightness of a surface covered with domes is not very different from one which is everywhere flat and horizontal.

The obvious type of feature to introduce is a hemispherical crater; however, the purely formal mathematical difficulties of integrating the differential brightness from various points of the crater when it is located off the luminance equator prevented the use of such a model. The type of structure finally adopted was a cylindrical depression whose axis is everywhere parallel to lines of luminance longitude. Such a feature is not as artificial as it may at first sight appear due to the special property of Eq. (6) of being independent of effective latitude. If a surface is tilted in such a manner as to change only its apparent latitude its brightness will be unchanged; only a tilt which alters its apparent

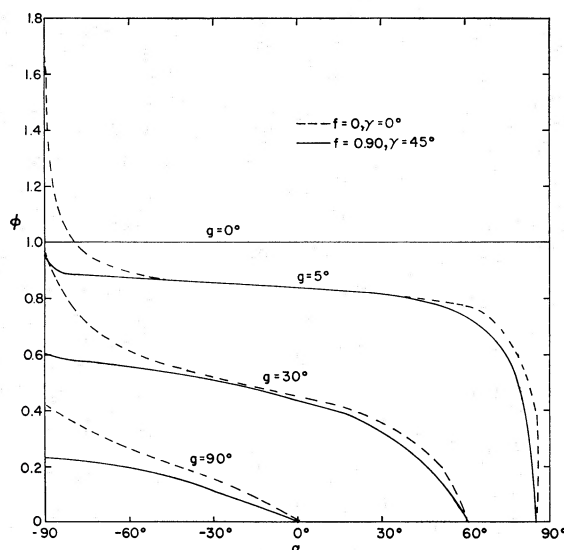


FIG. 3. Theoretical photometric function versus luminance longitude for several values of phase angle. Dashed curves: old theoretical function; solid curves: improved function.

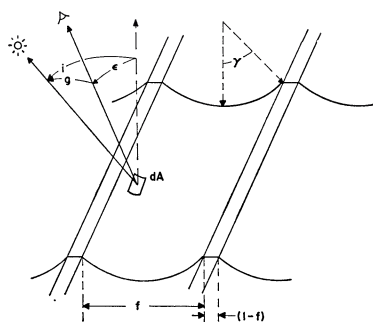


FIG. 4. Photometric model of the lunar surface. The surface material is open and porous.

longitude will change its brightness. Thus the variation in brightness of a spherical cavity will be similar to that of a short section of cylindrical trough, provided both are covered with a material having a differential photometric function of the type described by Eq. (6). The main difference will be due to variances in the details of the shadows cast within the structures by their rims. However, since for a material with a lunar type of photometric function the brightness is determined largely by the small-scale porous structure and not by the large-scale topography, the effects of shadow differences will be small.

The model adopted is shown in Fig. 4. A fraction  $f$  of the surface is assumed to be occupied by cylindrical depressions whose axes are aligned with lines of longitude. The half-angle of the depressions is  $\gamma$ ; that is,  $\gamma$  is the maximum departure of the slope of the local surface from the horizontal. The areas between depressions are flat and horizontal. All portions of the surface are assumed to have the brightness law given by Eq. (6).

The integration of Eq. (6), using (7) and (8), over those portions of the surface of Fig. 4 which are both

visible and illuminated is straightforward. The result is that the brightness  $E$  is given by Eqs. (1) and (2) in which  $\Sigma$  and  $B$  are unchanged but in which the form of  $L$  has been replaced by the following function:

$$L(\alpha, g) = \left\{ K_1 \frac{1-f}{1 + \cos\alpha / \cos(\alpha+g)} + K_2 \frac{f}{2 \cos \frac{1}{2}g \cos\alpha \sin\gamma} \right. \\ \times \left[ \cos(\alpha + jg) \sin(\gamma + kg) \right. \\ \left. \left. - \frac{1}{2} \sin^2 \frac{1}{2}g \ln \left| \frac{\cos(\alpha + jg) + \sin(\gamma + kg)}{\cos(\alpha + jg) - \sin(\gamma + kg)} \right| \right] \right\}, \quad (11)$$

where  $K_1$ ,  $K_2$ ,  $j$  and  $k$  have different values depending on  $\alpha$  and  $g$ : the  $(\alpha, g)$  plane is divided into six regions, which are shown in Fig. 5, and the values of  $K_1$ ,  $K_2$ ,  $j$ , and  $k$  in each region are given in Table I.

TABLE I. Constants for use with Eq. (11).<sup>a</sup>

Region	Definition	$K_1$	$K_2$	$j$	$k$
0	$-\frac{1}{2}\pi \leq \alpha \leq \frac{1}{2}\pi, (\frac{1}{2}\pi - \alpha) \leq g \leq \pi$	0	0	...	...
1	$(-\frac{1}{2}\pi + \gamma) \leq \alpha \leq \frac{1}{2}\pi, (\frac{1}{2}\pi - \gamma - \alpha) \leq g \leq (\frac{1}{2}\pi - \alpha)$	1	1	1	$\frac{1}{2}$
2	$(-\frac{1}{2}\pi + \gamma) \leq \alpha \leq (\frac{1}{2}\pi - \gamma), 0 \leq g \leq (\frac{1}{2}\pi - \gamma - \alpha)$	1	1	$\frac{1}{2}$	0
3	$-\frac{1}{2}\pi \leq \alpha \leq (-\frac{1}{2}\pi + \gamma), 0 \leq g \leq (\frac{1}{2}\pi - \gamma - \alpha)$	1	1	0	$\frac{1}{2}$
4	$-\frac{1}{2}\pi \leq \alpha \leq (-\frac{1}{2}\pi + \gamma), (\frac{1}{2}\pi - \gamma - \alpha) \leq g \leq (\pi - \gamma)$	1	1	$\frac{1}{2}$	1
5	$-\frac{1}{2}\pi \leq \alpha \leq (-\frac{1}{2}\pi + \gamma), (\pi - \gamma) \leq g \leq (\frac{1}{2}\pi - \alpha)$	1	0	...	...

<sup>a</sup> Only values appropriate to  $g \geq 0$  are given explicitly in this paper. The photometric function is symmetric with respect to a simultaneous change of sign of  $\alpha$  and  $g$ .

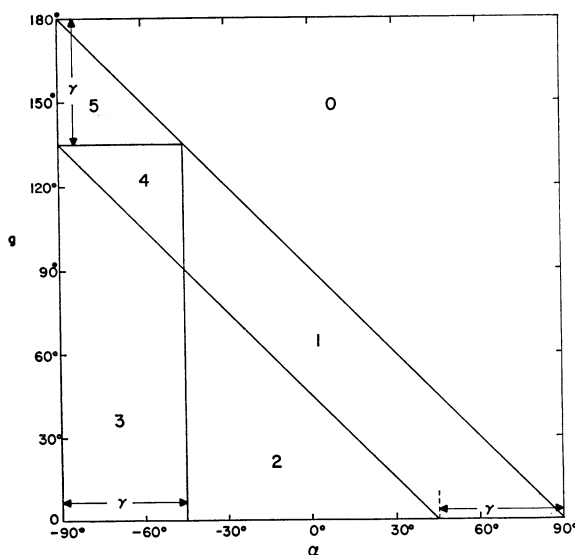


FIG. 5. Regions in  $(\alpha, g)$  plane for use with Table I in Eq. (11). See note to Table I.

The new photometric function contains three independent parameters,  $h$ ,  $f$ , and  $\gamma$ , which must be fitted to the observations. The data fitted were those of Fedoretz (1952), as reduced to averaged relative brightness contours by Herriman, Washburn, and Willingham (1963) of the Jet Propulsion Laboratory. Preliminary estimates of these parameters were obtained as follows. It was noted that for areas near the center of the disk  $\phi$  is relatively independent of  $f$  and  $\gamma$ ; that is, for areas observed nearly normally, the manner in which brightness varies with phase depends primarily on the microrelief and porosity of the surface and is only slightly affected by the larger scale depressions. This fact is illustrated in Fig. 3, where  $\phi$  is shown for  $f=0, \gamma=0$  and for  $f=0.9, \gamma=45^\circ$ . Hence to determine  $h$  the function with  $f=0, \gamma=0$ , was fitted by eye to the JPL curve at  $\alpha=0$ . This gave  $h=0.40 \pm 0.05$ .

The corrected expression for  $L$  has a particularly simple limiting form near the limb, which is fortunate since the corrections are most important in these regions. Thus  $f$  and  $\gamma$  were determined simultaneously by eye-fitting the theoretical expression with  $h=0.04$  to the JPL curves at the limb. This gave  $f=0.90 \pm 0.05$  and  $\gamma=45^\circ \pm 5^\circ$ . The estimates of error are subjective estimates only. This procedure is subject to criticism on the grounds that very few observations exist for areas on the limb and the JPL curves are extrapolations

from smaller values of  $\alpha$ . However, visual observations do not indicate anything photometrically unique about the limb regions, and such an extrapolation is probably reasonably valid (Minnaert 1962).

The improved photometric function is shown in Fig. 6 along with the JPL curves. The main differences between the two sets of curves are seen to lie near the terminator where, again, there are few data points available but where, now, extrapolation is difficult because the brightness changes rapidly. The improved function is also plotted in Figs. 7 and 8 along with data points of Fedoretz as corrected for normal albedo by Parker *et al.* (1963). The agreement between the observations and the theory is seen to be quite reasonable.

### C. Opposition Effect

It has long been realized that the brightness of the moon increases sharply very close to full moon. Recently Gehrels and his co-workers (Gehrels, Coffeen, and Owings 1964) have shown that the intensity of reflected

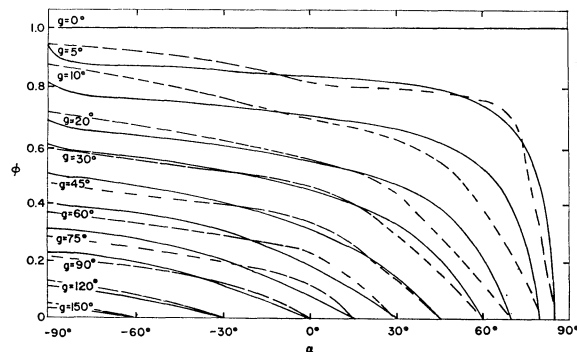


FIG. 6. Photometric function versus luminance longitude for various phase angles. Solid curves: theoretical function of this paper; dashed curves: empirical JPL function of Heriman *et al.* (1963), based on data of Fedoretz (1952). See note to Table I.

sunlight at  $0^\circ 5'$  phase angle is over 25% greater than at  $5^\circ$  phase angle. This "opposition effect" has been confirmed by Van Diggelen (1965). Oetking (1965) has recently observed that a large number of terrestrial materials display a similar brightness surge, although the effect is generally less pronounced than for the moon. The cause of the opposition effect is at present rather obscure. Lunar soil particles may reasonably be supposed to be of irregular size, shape, and orientation, and there appear to be no reasons to expect such a sharp, narrow peak in the average scattering patterns of such particles. The diffraction pattern of a particle large compared with the wavelength of light may be quite narrow, but this peak is in the forward direction only. While certain optically perfect objects, such as corner reflectors or spheres could in principle account for the opposition effect it is unreasonable to expect the entire lunar surface to be covered with them, and in any case they would not long retain their required

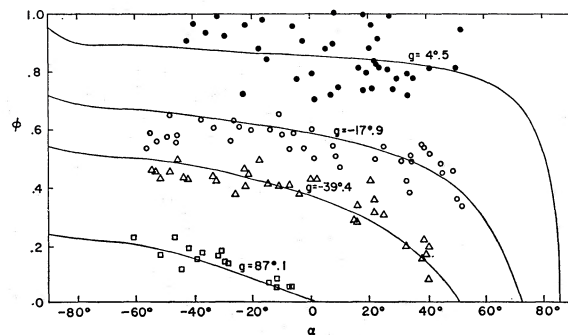


FIG. 7. Normalized brightness of lunar surface areas as a function of longitude for several phase angles. Solid line: theoretical photometric function of this paper; points: data of Fedoretz (after Parker *et al.* 1964). See note to Table I.

degree of optical perfection under micrometeorite bombardment.

The obvious remaining explanation is that the brightness surge is due to the effects of shadow-casting and is thus in the same category of phenomena as the backscatter effect discussed previously. Indeed, Gehrels, Coffeen, and Owings (1964) were able to fit their data by the photometric function of Paper I with  $h=0.05$ , where  $h$  is the parameter in the retrodirective function  $B(g)$  [Eq. (3)]. However, while using  $h=0.05$  gives agreement between theory and observation for phase angles less than about  $20^\circ$  an unacceptable discrepancy is introduced for larger phase angles.

The opposition effect can be introduced into the present theory in a rather natural manner if it is assumed that the particles of the lunar soil are not simple, dense grains having largely convex surfaces, but are instead extremely porous and irregular. Gault and his co-workers (Gault *et al.* 1964) have produced such particles by hypervelocity impact into a porous medium (pumice). Also, anyone who has worked with powders in which the average particle size is a few microns or less is aware that the common tendency of such powders is to form porous clumps consisting of many thousands of smaller particles. This clumping is

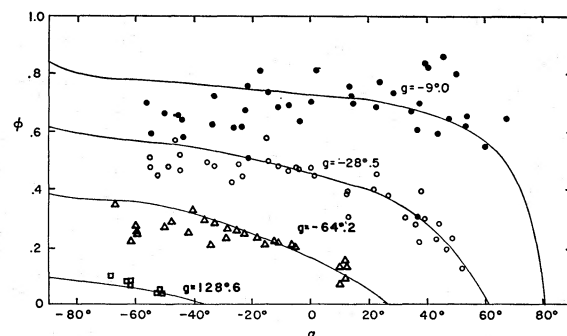


FIG. 8. Normalized brightness of lunar surface areas as a function of longitude for several phase angles. Solid line: theoretical photometric function of this paper; points: data of Fedoretz (after Parker *et al.* 1964). See note to Table I.

due to the intermolecular adhesive forces which act between grains.

On the model proposed here the opposition effect is presumed to arise by shadowing within the different portions of a complex particle. Hence the effect can be introduced into the theoretical photometric function through altering the form of  $\Sigma$ . The individual particle of the model now consists of subunits randomly arranged into a structure of high porosity; thus the form of the average scattering function of such a particle will be very similar to Eq. (9) for the integrated brightness of the moon plus a term to take forward-scattering into account. The new form proposed for  $\Sigma$  is:

$$\Sigma(g) = \frac{1}{2} \{ [1 - \sin^{\frac{1}{2}} |g| \tan^{\frac{1}{2}} |g| \ln(\cot^{\frac{1}{4}} |g|)] \sigma(g) B(g) + 0.1(1 - \cos |g|)^2 \}, \quad (12)$$

where  $B(g)$  is given by Eq. (3) with  $h=0.05$ , and  $\sigma(g)$  is the average scattering function of a subunit of the clump (the factor  $\frac{1}{2}$  is for normalization). The function

$$[1 - \sin^{\frac{1}{2}} |g| \tan^{\frac{1}{2}} |g| \ln(\cot^{\frac{1}{4}} |g|)] + 0.1(1 - \cos |g|)^2$$

has been plotted as curve  $B$  of Fig. 2; it may be noticed that this curve is quite close to curve  $A$ , which is a plot of Eq. (4), the original form of  $\Sigma$ . From Fig. 1 it is seen that the curve of  $B(g)$  with  $h=0.05$  is close to unity except for phase angles less than about  $5^\circ$ , where the brightness suddenly doubles. Hence, if form (12) is used for  $\Sigma$  with  $h=0.05$  and  $\sigma(g)=1$ , the resulting photometric function will be virtually unchanged (apart from the factor  $\frac{1}{2}$ ) from that shown in Figs. 6, 7, and 8 except for a surge in brightness for phase angles smaller than about  $5^\circ$ . Setting  $\sigma(g)=1$  implies that the subparticles are isotropic scatterers, which is reasonable for small, irregular, translucent grains.

### III. DISCUSSION

The theoretical lunar photometric function proposed in Paper I, which describes the variation of brightness of areas over most of the lunar disk, has been modified so that it more nearly agrees with observations of limb areas. The new photometric function is given by Eq. (2), whose components are given by Eqs. (3), (4), and (11), and Table I. The modification consists of replacing Eq. (5) by Eq. (11). These expressions contain three fitable parameters  $h$ ,  $f$ , and  $\gamma$ ;  $h$  is related to the porosity of the lunar soil and governs the sharpness of the backscatter peak;  $f$  is the fraction of the surface occupied by depressions;  $\gamma$  is the effective maximum angle which the walls of the depressions make with the local horizontal. Best preliminary values of these parameters are  $h=0.40$ ,  $f=0.90$ ,  $\gamma=\sin 45^\circ$ . The opposition effect can be included, if desired, by replacing Eq. (4) by Eq. (12) in which  $h=0.05$  and  $\sigma(g)=1$ . These parameters are averages for the entire lunar surface.

Undoubtedly, more precise values for the parameters could be obtained. However, the primary purpose of this paper is to demonstrate the ability of the model to predict the phase variations of lunar surface brightness and to infer certain properties of the moon's surface from the model. It was felt that a minor improvement in fit would not justify the additional effort involved, especially in view of the scatter of data of Figs. 7 and 8.

The data scatter is due to at least two factors. (1) Fedoretz's points were obtained using photographic techniques with the attendant calibration difficulties. To attain more accurate values for the photometric parameters the results of photoelectric measurements, such as those by Wildey and Pohn (1964), should be utilized. (The Wildey and Pohn measurements were not used in this paper because of the limited range of phase angles observed.) (2) The data of Figs. 6, 7 and 8 combine observations of a large variety of areas on the moon, whereas the photometric function of the lunar surface shows a slight dependence on stratigraphy and type of terrain. Hence the exact values of the parameters will depend on the area examined.

Equation (12) is based on a model which assumes that the opposition effect is due to shadowing within complex, porous clumps of lunar rock powder; however, the author does not wish to assert the correctness of this model strongly, particularly in view of Oetking's (1965) findings that less complicated surfaces also display the opposition effect. The use of Eq. (12) is proposed mainly because it correctly describes the effect and also because it can be introduced into the theoretical photometric function without making assumptions which are unnatural and *ad hoc*.

The remainder of the model on which the function is based is felt to be a realistic representation of the lunar surface. The small-scale morphology of the surface of the moon is presumed to be one in which particles (or porous clumps of particles) of lunar soil are arranged into an open, porous lattice which is optically thick. The surface formed by this porous layer is not flat, but is warped into a multitude of steep-sided structures. Purely for reasons of mathematical simplicity these structures are taken to be cylindrical depressions whose axes are aligned with lines of luminance longitude. However, the primary requirement is that, even when viewed from a direction nearly parallel to the ground, many areas are visible which contain a large component of tilt in the direction of the observer; any surface having similar topological properties will possess a similar photometric function.

The size of these structures on the lunar surface is estimated to be of the order of a few centimeters and smaller, judging from the radar-scattering behavior of the moon at short wavelengths (Evans and Hagfors 1964). Although the radar data allow an estimate of the scale of the structures, they are not able to specify many details of shape other than that the surface is rougher than at longer wavelengths. From the photo-

metric model it is possible to reject a topology which is dominated by convex-upward structures, such as domes, ridges, or boulders, since when such a surface is viewed at glancing angles mainly the tops of the domes are visible and these are nearly horizontal. The dominant morphology of the surface is probably concave-upward.

The most likely nature of the structures is that they are primary and secondary impact craters and impact debris. This picture of the lunar surface would be consistent with the Ranger photographs, except that on the scale of meters and larger which can be resolved by Ranger the surface is far less than 90% covered with craters, and slopes as high as  $45^\circ$  are extremely rare. However, Shoemaker (1965) estimates that on a scale of centimeters and millimeters the lunar surface is saturated with craters and debris from impacts of primary and secondary meteorites. Also, on a large scale the soil is likely to be essentially cohesionless, and slumping and soil creep will prevent the preservation of slopes larger than the angle of repose of the material. But on a small scale even a moderate amount of cohesion in the soil would allow highly tilted surfaces to be common. The value of  $45^\circ$  for  $\gamma$  is some sort of a weighted average of the slopes visible at glancing angles and, hence, surfaces with tilts larger than  $45^\circ$  are probably common. The picture of the lunar surface which emerges from this discussion is a landscape somewhat reminiscent of a sandy beach after a rain-storm: that is, on a scale of meters and larger the surface is smooth and undulating with relatively gentle slopes and an occasional crater, but on a scale smaller than a few centimeters the surface is completely covered with craters and ejecta splatter patterns.

A possible alternative to the nature of the small-scale roughness has been proposed by T. Gold (private communication), who suggests that these features are erosion patterns built by electrodynamic processes acting on the lunar dust. The relevant scale length of possible electrical transport mechanisms would be that of the electric field due to photoelectrons ejected from the lunar surface, which would be of the order of centimeters. On a scale large compared with the photoelectric charge layer height, transport would act to smooth the surface, but on a scale small compared with this height, complex patterns due to local electrical and topological conditions could cause considerable

roughness. Although this suggestion as to the nature of the roughness is considered to be much more speculative than is an impact morphology, it cannot at present be completely ruled out.

After this paper was submitted for publication the Luna 9 space station successfully soft-landed on the moon and transmitted pictures of a small area in the western part of Oceanus Procellarum back to earth. The small-scale features of the surface photographed by the station appear to consist primarily of crater-like depressions and piles of rubble, in agreement with the predictions of this paper. Thus, it is probable that the appearance of most of the lunar surface, including both highlands and maria, is similar to the Luna 9 landscape.

## ACKNOWLEDGMENTS

I thank Jane Lee for aid in making several of the calculations in this paper. This research was sponsored by the National Aeronautics and Space Administration under grant NsG-382.

## REFERENCES

- Evans, J. and Hagfors, T. 1964, *Icarus* 3, 151.  
 Fedoretz, V. 1952, *Publ. Kharkov Obs.* 2, 49.  
 Fessenkov, V. 1962, "Photometry of the Moon," in *Physics and Astronomy of the Moon*, Z. Kopal, Ed. (Academic Press, Inc. New York), pp. 99-130.  
 Gault, D., Heitowitz, E., and Moore, H. 1964, *Trans. Am. Geophys. Union* 45 (1), 74.  
 Gehrels, T., Coffeen, T., and Owings, D. 1964, *Astron. J.* 69, 826.  
 Hapke, B. 1963, *J. Geophys. Res.*, 68, 4571-4586 (Paper I).  
 —. 1965a, on *Ann. N.Y. Acad. Sci.* 123, 711.  
 —. 1965b, "Optical Properties of the Moon's Surface," in *Proceedings of the Conference on the Nature of the Lunar Surface* (to be published).  
 Hapke, B., and VanHorn, H. 1963, *J. Geophys. Res.* 68, 4545.  
 Herriman, A., Washburn, H., and Willingham, D. 1963, "Ranger Preflight Science Analysis and the Lunar Photometric Model," *Jet Propulsion Laboratory Tech. Rept.* No. 32-384 (Rev.).  
 Minnaert, M. 1962, "Photometry of the Moon," in *Planets and Satellites*, G. Kuiper and B. Middlehurst, Ed. (University of Chicago Press, Chicago), pp. 213-248.  
 Oetking, P. 1965, *Trans. Am. Geophys. Union* 46, (1), 131.  
 Parker, H., Mayo, T., Birney, D., and McCloskey, G. 1964, "Evaluation of the Lunar Photometric Function," *Univ. Virginia Res. Lab. for Eng. Sci. Rept.* No. AST-4015-101-64U.  
 Rosenberg, D., and Wehner, G., 1964, *J. Geophys. Res.* 69, 3307.  
 Shoemaker, E. 1965, "Preliminary Analysis of the Fine Structure of the Lunar Surface," in "Ranger VII, Part II. Experimenters' Analyses and Interpretation," *Jet Propulsion Lab. Tech. Rept.* No. 32-700, pp. 75-134.  
 Van Diggelen, J. 1958, *Rech. Astron. Obs. Utrecht* XIV(2).  
 —. 1965, *Planetary Space Sci.* 13, 271.  
 Wildey, R., and Pohn, H. 1964, *Astron. J.* 69, 610.